JOTCS A
Journal of the Turkish Chemical Society
Section: A
Chemistry
TURKISH CHEMICAL SOCIETY

Copper Oxide Nano Biochar from Spent Coffee Grounds for Phosphate Removal and its Application as an Antibacterially Active Entity

Biruk Bezabeh Yimam[1*], Gamada Begna Sisay[1], Eskedar Getachew Feleke[1]

[1]Chemistry Department, Mizan Tepi University P.O.Box 121, Tepi, Ethiopia

Abstract: From the viewpoint of both eutrophication and sustainable use of phosphate, the removal and recovery of phosphate from wastewater are important. Adsorption is seen as a viable alternative for effective phosphate removal, even at low concentrations. It is very simple to operate and cheaper. Among the various adsorbents tested, biomass-derived nanomaterials, such as nanobiochar, have shown promising efficiency. However, the use of pristine biochar is often less effective and difficult to recycle. In the present study, copper oxide-modified nanobiochar from spent coffee grounds is presented as an effective phosphate adsorbent. The adsorbent was prepared by the acid digestion of spent coffee grounds, followed by the co-precipitation of copper metal. The developed adsorbent was characterized by BET, FTIR, and XRD. Batch mode adsorption studies were conducted to assess the adsorption efficiency of the developed adsorbent and to investigate the effect of pH, initial concentration, contact time, and adsorbent dose. It was observed that acidic conditions favored the adsorption of phosphate, with maximum adsorption efficiency (93%) at pH 3. The maximum equilibrium phosphate adsorption capacity in this study was 50.2 mg/g at 25 °C, pH 3, a phosphate concentration of 20 mg/L, and an adsorbent dose of 35 mg/mL. The batch experimental data fit the Freundlich isotherm with regression (R^2 = 0.991), which signifies that the surface of the adsorbent is heterogeneous. Adsorption kinetic data were best fitted with the pseudo-second-order kinetic model (R^2 = 0.996), indicating that the adsorption process was dominated by chemisorption. The copper oxide nanoparticles and Cu/NBC showed relatively higher zone inhibition in gram-positive bacteria than in gram-negative bacteria at similar concentrations. This might be due to the higher activity of the nanoparticle extract on gram-positive bacteria, as most nanoparticle extracts were more active in gram-positive bacteria. This difference may be explained by the difference in the structure of the cell wall in gram-positive bacteria, which consists of a single layer, and in gram-negative bacteria, which has a multi-layered structure and is quite complex. In the majority of test bacteria, Cu/NBC showed better activity. The higher activity of this nanomaterial might be associated with the number of bioactive metabolites and their synergetic activities.

Keywords: Adsorption, Antibacterial activity, Copper oxide nano biochar, Phosphate, Spent coffee

Submitted: October 5, 2023. **Accepted**: February 13, 2024.

Cite this: Yimam BB, Sisay GB, Feleke EG. Copper Oxide Nano Biochar from Spent Coffee Grounds for Phosphate Removal and its Application as an Antibacterially Active Entity. JOTCSA. 2024;11(2):835-44.

DOI: https://doi.org/10.18596/jotcsa.1369920

***Corresponding author.** E-mail: birukbezabeh04@gmail.com

1. INTRODUCTION

Phosphorus is necessary for the growth of plants and is essential for all living things. Rock phosphate is a finite resource that is tapped into for fertilizer production, food production, and contemporary farming (1). Phosphate accumulates in water systems due to industrial and agricultural discharge. They can result in the phosphate enrichment of water bodies, which is occurring worldwide and is known as eutrophication (2). Hence, from the viewpoint of both eutrophication and sustainable use of phosphate, the removal and recovery of phosphate from wastewater, manure, and sludge are important (3).

To date, many different methodologies have been mapped out for the mitigation of aqueous phosphates, such as anion exchange (4), chemical precipitation, adsorption, etc. Chemical precipitation is the most commonly used technique; however, it is limited by the generation of large amounts of sludge; the separation of chemically bonded phosphate can be difficult and

costly; and it is unsuitable for small-scale plants (5). Adsorption is considered a promising alternative for the effective removal and recovery of phosphate, even at low concentrations (6). Hence, the design of an effective adsorbent with economic feasibility is very important. Various adsorbents, such as polymers (7), metal oxides/hydroxides (8), and biomass-derived adsorbents such as activated carbon and biochar (9), have been studied, and promising results have been reported.

The material mentioned in the above paragraph requires expensive raw materials for their preparation and difficulty in their operation. Therefore, establishing an economical adsorbent is imperative (10). In contrast, biochar, which is a carbon-rich biomass source formed by thermochemical conversation has elicited much attention due to its kindness to the environment and economics. For the present study, coffee grounds were selected as sources of biomass. However, most of the biochar has a low adsorption capacity for phosphate because of its anion-dominated surface. Hence, it's important to modify the biochar by converting macrobiochar to nanobiochar with size reduction followed by co-precipitation of cationic metals, such as Fe^{2+}/Fe^{3+}, Mg^{2+}, and Mg/Al, on the nanobiochar to enhance its affinity towards phosphate. Compared to pristine nanobiochar (NBC), metal-modified nanobiochar has the maximum phosphate adsorption capacity because the surface of the adsorbent becomes cations-dominated, which makes it suitable for upcoming phosphate. So in this study, copper oxide modifies the surface of nanobiochar made from coffee grounds.

Copper oxide nanoparticles and copper oxide nanoparticle nanobiochar (Cu/NBC) show strong antibacterial properties against pathogens. It can inhibit the growth of these microorganisms due to the damage they cause to the membrane of bacterial cells (11, 12). The application of nanomaterials as new antimicrobials should provide new modes of action and/or different cellular targets compared with existing antibiotics, which somehow promote multiple drug-resistant microbes (12). To the best of our knowledge, this is the first adsorbent reported by combining the nano-scale feature of biochar with copper metal modification.

The main objective of this study is to develop copper-modified nanobiochar from spent coffee grounds for phosphate recovery, and its antibacterial activity.

2. EXPERIMENTAL

2.1. Chemicals and Materials

Analytical-grade chemicals and reagents were all employed in this research project without further purification. Ammonium molybdate tetrahydrate (CAS 12054-85-2), $(NH_4)_6Mo_7O_{24}{\cdot}4H_2O$ 99%), copper nitrate hexahydrate (CAS 13478-38-1), $(Cu(NO_3)_2{\cdot}6H_2O$, 99%), potassium dihydrogen phosphate (CAS 7778-77-0), (KH2PO4, 98%), antimony potassium tartrate (CAS 28300-74-5), $(C_8H_4K_2O_{12}Sb_2{\cdot}3H_2O$, 99.5%), were purchased from Research Lab Fine Chemicals, Mumbai, India. Mueller-Hinton Agar (CAS 9002-18-0, MHA) and Dimethyl Sulfoxide (CAS 67-68-5, Hi-Media Laboratories Pvt. Ltd., India)

Characterization was performed by Brunauer – Emmett – Teller (BET) (SA-9600, USA), a Fourier transform infrared spectrometer (FT-IR, iS50ABX Thermo Scientific, Germany), an X-ray diffraction spectrometer (XRD-700 X-RAY, Germany), and a UV-Vis spectrophotometer (Biochrom, UK).

2.2. Preparation of Copper Oxide Nano Biochar

First, spent coffee grounds from nearby coffee shops were gathered, cleaned, and oven-dried. At various temperatures (250, 350, and 450 ^oC), the cleaned spent coffee grounds were treated to gradual pyrolysis in a muffle furnace. To create uniform-sized particles, the obtained biochar was mashed in a mortar and pestle and sieved using a 150.0 m mesh (5, 13). The size of the biochar particles was reduced by acid digestion in a hydrothermal autoclave reactor. The process was typically allowed to finish in a fume hood after 1.0 g of the resulting biochar was put into a hydrothermal autoclave reactor holding 60.0 mL of concentrated HNO_3 and H_2SO_4 (1:3 ratio). Finally, the product was collected, filtered, washed, and stored for further experiments (1,5). The co-precipitation of metal ions allowed for the modification of nanobiochar. Typically, 200.0 mL of solutions containing $CuSO_4{\cdot}6H_2O$ (0.2 M) in a 2:1 ratio were added to 0.4 g of nanobiochar. After that, 1.0 M NaOH was added drop by drop while being stirred rapidly for 1 hr. After allowing the reaction mixture to sit for 24 hrs, the precipitate was ultimately removed, cleaned, and kept for later investigations as shown in Figure 1(13).

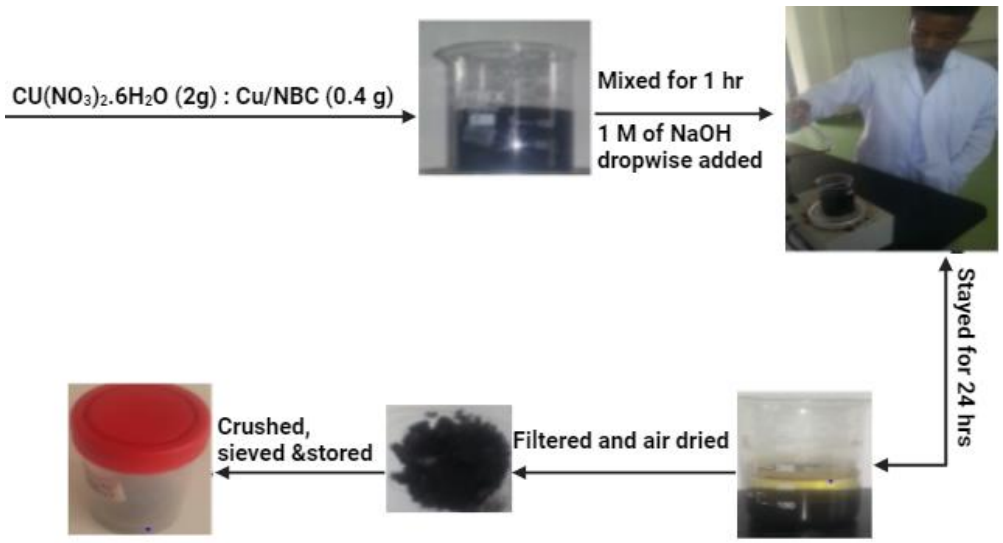

Figure 1: The schematic representation of the preparation of Cu/NBC.

2.3. Adsorption study

In batch-mode adsorption studies, the material capacity for phosphate adsorption was evaluated. In a series of batch mode tests, factors affecting the efficiency of the adsorption, such as pH (3–12) and a dose of adsorbent (15–35 mg), were investigated using the one factor-at–a-time approach. Quantification of the residual phosphate concentration was measured by the ascorbic acid method (Method, 1978) using a calibration curve from phosphate external standards (1, 11, 12, 14). The removal efficiency and the amount of phosphate adsorbed were determined by using equations (1) and (2), respectively.

$$\% \text{ removal} = \frac{C_o - C_f}{C_o} * 100 \quad \text{(Eq. 1)}$$

$$\text{Adsorption capacity} = \frac{C_o - C_f}{\frac{V}{m}} \quad \text{(Eq. 2)}$$

Where C_o and C_f are the initial and final phosphate concentrations, qt is the amount of phosphate adsorbed at time t, V is the volume solution, and m is the mass of the adsorbent used. The adsorption isotherm was done by fitting the equilibrium data into the linear form of the Langmuir (Eq. (3)) and Freundlich (Eq. (4)) isotherm models.

$$q_e = \frac{q_m k_l C_e}{1 + k_l C_e} \quad \text{(Eq. 3)}$$

$$q_e = k_f C_e^{\frac{1}{n}} \quad \text{(Eq. 4)}$$

where q_e (mg $g^{-1)}$ and C_e (mg L^{-1}) are equilibrium adsorption capacity and equilibrium concentration, respectively; 1/n is the intensity of adsorption; K_f (mg g^{-1}) (Lmg^{-1})1/n is the Freundlich adsorption constant; q_m (mg g^{-1}) is the maximum adsorption capacity; and K_L (L mg^{-1}) is a Langmuir constant (12). Similarly, the kinetics study was done by fitting the equilibrium data into pseudo-first (Eq. (5)) and second-order (Eq. (6)) kinetic models shown below.

$$q_e = q_e(1\text{-}e^{k_1}t) \quad \text{(Eq. 5)}$$

$$q_e = \frac{k_2 q_e^2}{1 + k_2 q_e t} t \quad \text{(Eq. 6)}$$

Where q_e and q_t (mg g^{-1}) are the amounts of phosphate adsorbed at equilibrium and at time t, respectively; k_1 (min^{-1}), and k_2 (g $mg^{-1}min^{-1}$), are the rate constants of the corresponding models.

2.4. Antibacterial analysis of copper-modified nano biochar

2.4.1. Bacterial test organisms and standard antibacterial disc

The standard American Type Cell Culture (ATCC) bacterial species of Salmonella typhi, Escherichia coli, Staphylococcus aureus, and Streptococcus pneumoniae were obtained from the Department of Biology at Mizan-Tepi University, Ethiopia. The standard antibacterial disc used for the study was gentamicin.

2.4.2. Antibacterial activity

The Mueller-Hinton Agar (MHA) used was made according to previously reported literature (15–17), which called for mixing 38.0 g of powder media with 1.0 L of distilled water, sealing the mixture in a container, and autoclaving it at 121°C for 15 minutes. After that, the media were put on sterilized Petri dishes. After the media had solidified, 100.0 mL of the working stock culture was distributed with a sterile cotton swab, and stainless steel cork borer wells were formed in each Petri dish. Then different concentrations of nano copper oxide particles and nanobiochar (100 µg/mL, 250 µg/mL, and 500 µg/mL) were prepared by dilution of the stock solution in DMSO (negative control) and poured into the well using a micropipette. The plates were incubated for 24 hours at 37°C (16, 17). The extracts were tested in triplicate, and the findings were shown as the

mean standard deviation. The diameter of the zone of inhibition was measured in millimeters (mm).

3. RESULT AND DISCUSSION

3.1. Preparation and Characterization of Cu/NBC

The nanobiochar was obtained by first optimizing pyrolysis and then acid digestion. Co-precipitation modifies it with copper metal. Table 1 represents the nitrogen adsorption and desorption isotherms of adsorbents at room temperature. As shown in the table, the copper modification considerably increased the adsorbent's specific surface area. Since the specific surface area refers to both the total surface pore and external surfaces, the obtained result shows that Cu/NBC is more favorable for the adsorption process and antibacterial.

Table 1: BET Specific Surface Area of the nano biochar from nano biochar and after Cu^{2+} modification.

Adsorbent	BET (m^2/g)
NBC	7.09
Cu^{2+}/NBC	124.9

XRD was used to determine the crystallinity of the prepared adsorbent material. The peaks at 32.06°, 35.69°, 38.996°, and 48.93°, corresponding to (110), (002), (111), and (202) planes, can be assigned to the monoclinic structure of CuO (JCPDS, file no. 801268), respectively, as shown in Figure 2.b. The broad peak is centered at 24.5°, indicating the amorphous carbon phase in the nano-biochar, as shown in Figure 2.a. Hence, the XRD study confirms the availability of crystalline metallic phases of Cu on the adsorbent.

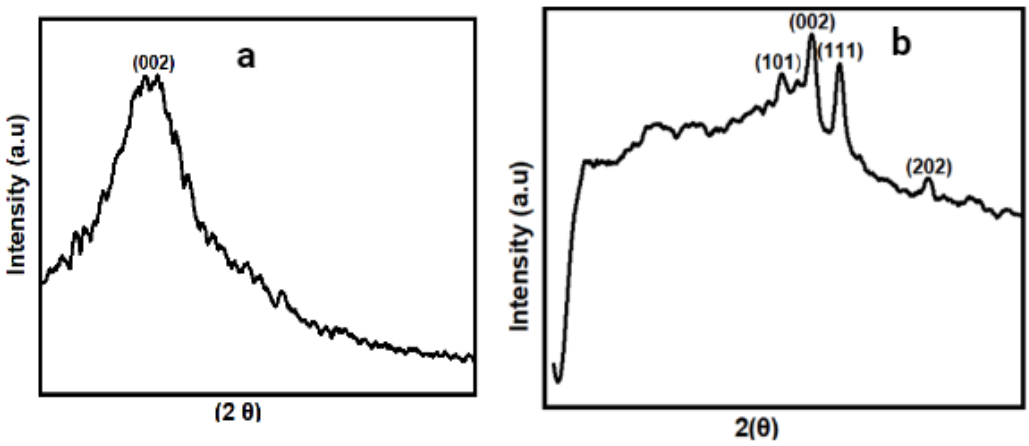

Figure 2: XRD peaks of (a), NBC; (b), CuO/NBC.

The surface functional groups involved were checked by FTIR (Fig. 3a–c). As seen in Fig. 3a, the FTIR spectrum of the NBC consists of absorption bands at 1716 cm^{-1}, 1546 cm^{-1}, and 1156 cm^{-1} which correspond to C=O, C=C, and C-O stretching vibrations, respectively. After modification, a peak appears at 602 cm^{-1} which corresponds to the CuO (Fig. 3c). This is in agreement with the XRD data and shows that the metal is successfully loaded on the NBC surface. After adsorption, two new bands appear at 1163 cm^{-1}, and 765 cm^{-1} which can be assigned P-O stretching and P-O-P bending modes, respectively (1).

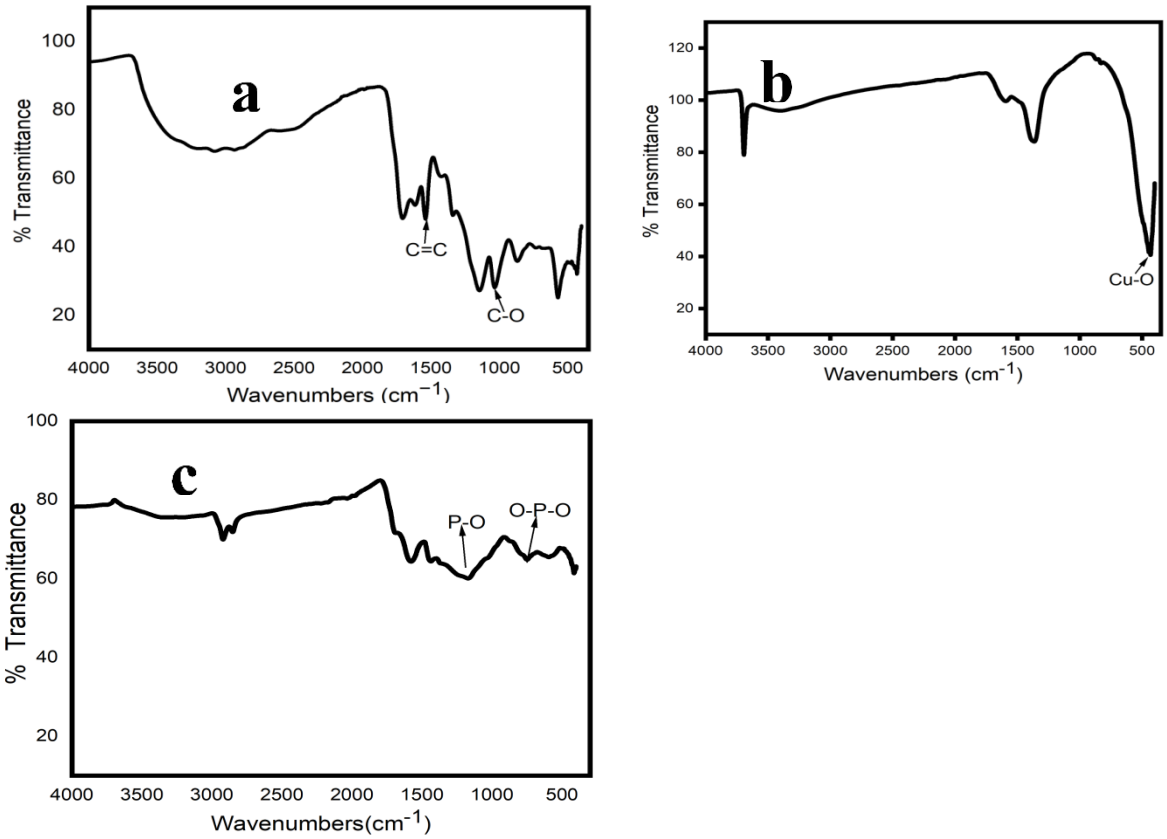

Figure 3: FTIR spectra of the adsorbents (a) NBC ; (b)Cu/NBC before adsorption ; (c) Cu/NBC after adsorption.

3.2 Adsorption Studies

The effect of pH, dose of adsorbent, contact time, and initial concentration on the adsorption efficiency was systematically studied in a batch-mode adsorption study by varying one factor at a time. The effect of pH on the adsorption of phosphate was studied by varying the pH of the solution from 3–12 while fixing other parameters. As shown in Fig. 4a**,** the phosphate removal efficiency reached its maximum (93%) at pH 3. The maximum adsorption capacity at pH 3 suggests that, in addition to the electrostatic attraction, there is precipitation of copper phosphate. This is because, for pH less than 2, H_3PO_4 and $H_2PO_4^{-1}$ are dominant species that trigger the precipitation of copper phosphate (18). This trend obtained is in agreement with previous studies on phosphate removal by Mg/Zr-spent coffee nano biochar adsorbents (Sisay *et al.).* Figure 4b shows the percentage of phosphate removal at various adsorbent doses. As seen in the figure, the percent removal increased with the adsorbent dose and reached its optimum (96.2%), and 19.24 mg/L of phosphate adsorbed at 35 mg of Cu/NBC, indicating that 35 mg of Cu/NBC could effectively remove 20 mg/L phosphates at pH 3. The increase in adsorption efficiency with an adsorbent dose can be attributed to the availability of additional active sites that could take up the phosphate anions.

The effect of contact time on phosphate adsorption by Cu/NBC was investigated by varying the contact time from 25- 100 minutes in batch mode adsorption experiments. As shown in Figure 4.d the adsorption process was very fast initially with more than 98 % of the adsorbate being removed in 25 minutes. The % removal continued to increase and started to stabilize after 85 minutes of contact time suggesting the attainment of the adsorption equilibrium. Thus 85 minutes is the optimal time for the study. The effect of initial concentration on the adsorption process was studied by conducting batch mode experiments at different initial concentration levels of phosphate (10-50 mg/L) while maintaining the rest three parameters constant. As shown in Figure 4.c the percent of adsorption was found to decrease with an increase in the initial concentration of adsorbate.

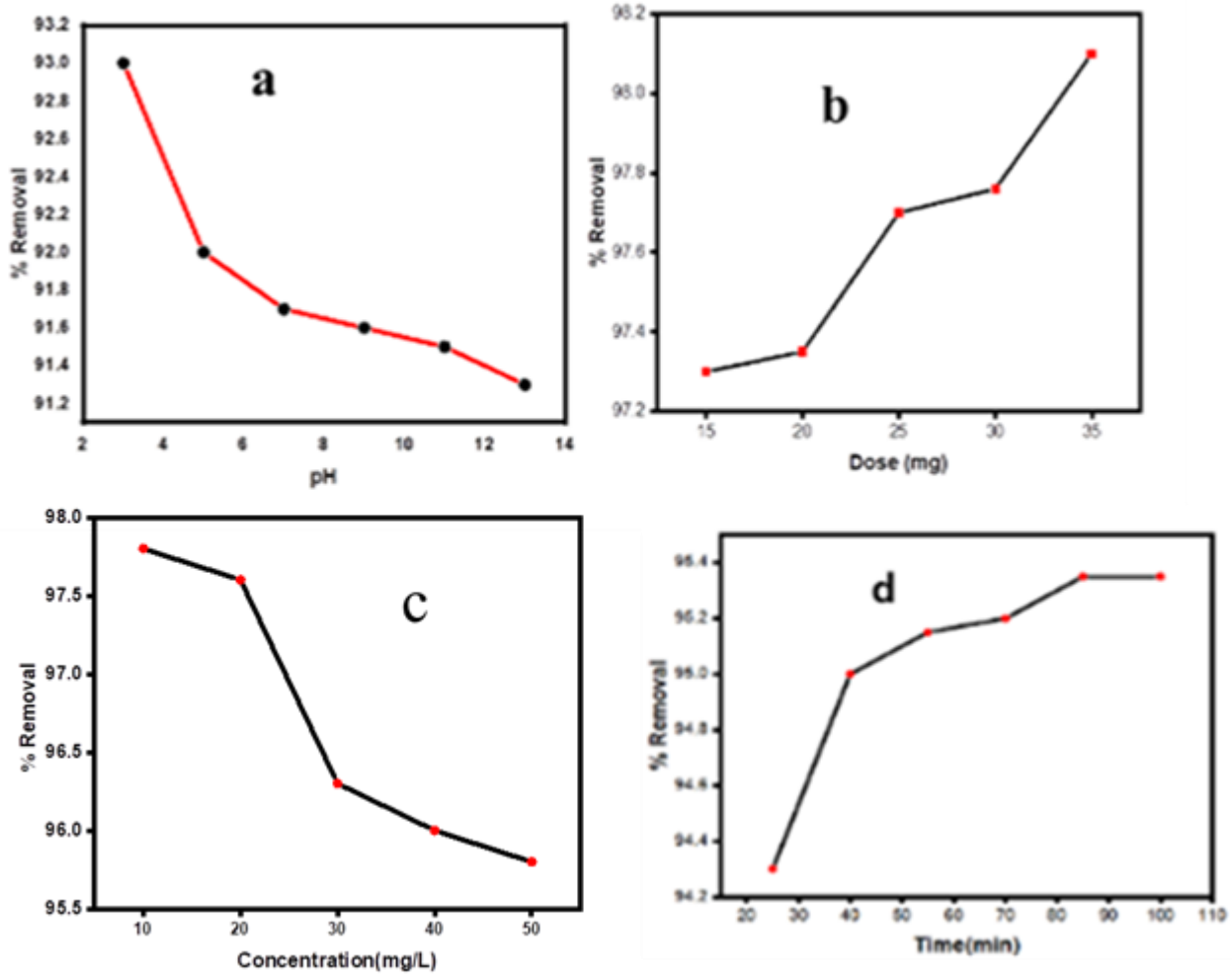

Figure 4: Effect of (a) pH; (b) effect of dose ; (c) initial concentration; and (c) effect of contact time of adsorbent on the adsorption efficiency.

3.2.1 Adsorption isotherm

The equilibrium data obtained at different phosphate concentrations (10–50 mg/L) at a fixed mass of adsorbent were fitted into Langmuir and Freundlich adsorption isotherm models (equations 3&4 respectively). As seen in Fig. 5a-b and Table 2, the Freundlich isotherm model better conforms to the equilibrium data ($R^2 = 0.991$).

Table 2: Freundlich and Langmuir Adsorption Parameters for PO_4^{3-} adsorption on Cu/NBC.

Langmuir model			Freundlich model		
K_L (L/mg)	q_m(mg/g)	R^2	K_F (mg/g)	N	R^2
1.57	142.9	0.984	50.2	1.27	0.991

The above results suggest that the adsorption of phosphate on Cu/NBC follows the heterogeneous surface and multilayer adsorption process.

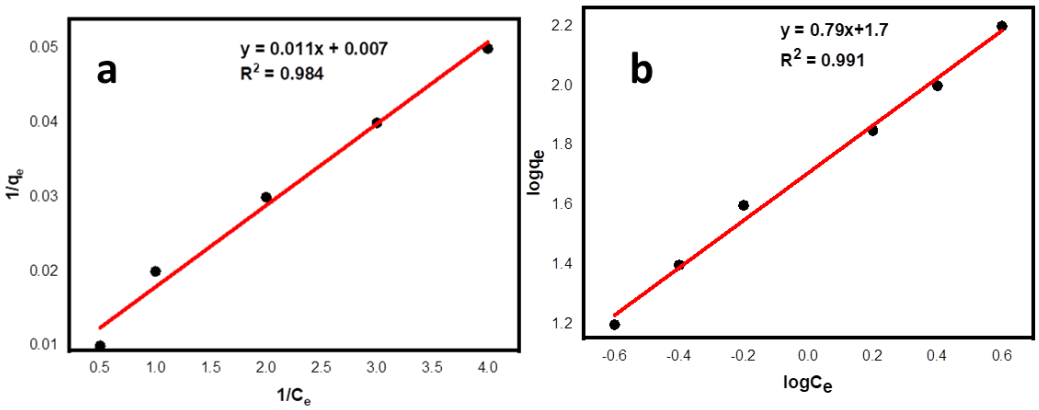

Figure 5: Phosphate adsorption isotherm of Cu/NBC; (a) Langmuir adsorption ;(b) Freundlich isotherm model.

3.2.2. Adsorption kinetics

As shown in Table 3, and Figure 6 the pseudo-first-order kinetic model is not applicable, since the correlation coefficient (R^2 = 0.952) obtained with this approximation is relatively low and the calculated q_e, values did not match the experimental q_e values well. This is because near equilibrium the experimental data deviate notably from the previous data obtained during the first stage of the experiment(19). The correlation coefficient obtained with the pseudo-second-order is, however, much higher (0.996), and the calculated q_e values show a good agreement with the experimental q_e values as seen in Table 3.

Table 3: Pseudo first order and Pseudo second order parameters for PO_4^{3-} adsorption on Cu/NBC.

Pseudo first order				**Pseudo second order**			
q_e exp (mg/g)	q_e, cal (mg/g)	k_1 (min^{-1})	R^2	q_e, exp (mg/g)	q_e, cal (mg/g)	K_2 (g/mg min)	R^2
26.2	0.06	0.05	0.952	26.2	26.3	0.0987	0.996

The above results suggest that the adsorption process was mainly controlled by the chemical reaction process due to either the sharing or exchange of electrons, rather than mass transfer. In this study metallic-modified nanobiochars have an abundant active site this is the reason why chemisorption is the dominant mechanism. Similar results were reported in the study of phosphorus removal and recovery in phosphate by Mg/Zr nano biochar (1).

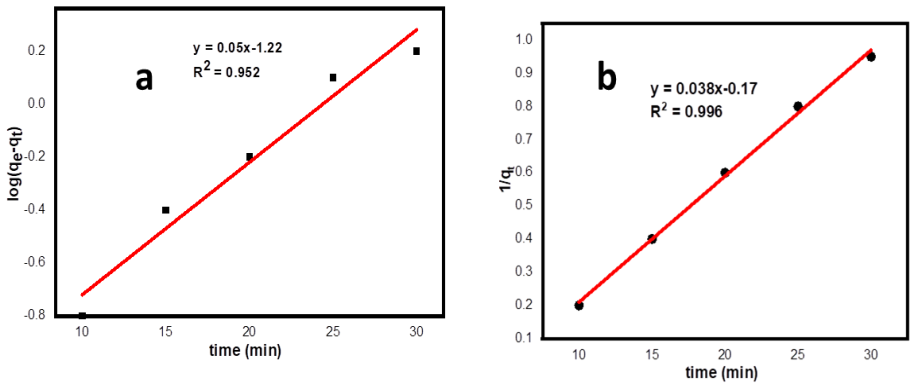

Figure 6: Adsorption kinetics of phosphate on Cu/NBC: (a) pseudo-first-order model; (b) pseudo-second-order model.

3.2.3. Comparison of Cu/NBC adsorption capacity with adsorbents

The adsorption capacity (mg/g) of Cu/NBC found in this study was compared with other metal-modified adsorbents for phosphate removal reported by other authors as shown in **Table 4**. It can be seen from the table that the Cu/NBC has by far better adsorption capacity than most of the recently reported materials for phosphate adsorption.

Table 4: The compassion of the adsorption capacity of Cu/NBC with other adsorbents.

S/N	Adsorbent	Adsorption capacity ($\frac{mg}{g}$)	Reference
1	Lanthanum-doped silica	47.89	8
2	Mg-biochar	14.33	20
3	Mg-Fe layered double hydroxides	16.31	21
4	Ca $(OH)_2$ -biochar	36.74	22
5	Magnetic Carbon Nanofibers	7.26	23
9	Mg-Zr NBC	39.4	1
10	Cu/NBC	50.2	This work

3.3. Antibacterial Analysis of Copper Oxide Nanoparticles and Nano Biochar

3.3.1. Antibacterial screening results

In this investigation, the antibacterial activities of copper oxide nanoparticles and Cu/NBC were evaluated using the agar well diffusion method at a concentration of 100, 250, and 500 µg/mL as shown in Table 5. The maximum zone of inhibition for the Cu/NBC was achieved for *S. aureus* at 17.31±0.19 mm at the concentration of 500 mg/mL, while the minimum antibacterial activity for the copper oxide nanoparticles for *S. typhi* and *E. coli* was obtained at 7.0±0.29 mm and 7.00±0.40 mm at a concentration of 10 mg/mL respectively.

The copper oxide nanoparticles and Cu/NBC have shown antibacterial activity based on the different concentrations that are explained in different literature (20,21). The copper oxide nanoparticles and Cu/NBC extract show greater antibacterial activity against gram-negative and gram-positive bacterial tests. The result is in agreement with the findings of, (20,21) who reported that *E.coil* and *S.typhi* were present respectively (Fig 7).

The copper oxide nanoparticles and Cu/NBC showed relatively higher zone inhibition in gram-positive bacteria than in gram-negative bacteria at similar concentrations. This might be due to the higher activity of the nanoparticle extract on gram-positive bacteria as most nanoparticle extracts were more active in gram-positive bacteria. This difference may be explained by the difference in the structure of the cell wall in gram-positive bacteria which consists of a single layer and the gram-negative bacteria, which is a multi-layered structure and quite complex (15-17).

Table 5: Antibacterial activities of copper nanoparticles and nano biochar against gram-negative and gram-positive bacteria.

		Concentration of extracts Zone of inhibition in diameter (mm)				
Test bacteria	Nanoparticles	100 µg/mL	250 µg/mL	500 µg/mL	(+) control	(-) control
S. typhi	CuO	7.0±0.29	8.19±0.70	10±0.33	15±0.59	NA
	Cu/NBC	9.21±0.39	11.21±0.29	13.44±0.30		
E. Coli	Cu	7.00±0.40	10.41±0.19	12.00±0.11	16.33±0.27	NA
	Cu/NBC	8.37±0.59	11.01±0.79	12.46±0.45		
S. Aureu	Cu	7.91±0.71	11.61±0.21	15.24±0.33	18.71±0.59	NA
	Cu/NBC	10.25±0.33	13.51±0.35	17.31±0.19		
S. pneumoniae	Cu	7.21±0.45	12.3±0.33	14.19±0.27	19.82±0.47	NA
	Cu/NBC	11.45±0.35	14.21±0.72	17.38±0.56		

Values are expressed as mean ± SD (n = 3). NA = no activity, (+) control (gentamicin), and (-) control = negative control (DMSO).

In the majority of test bacteria, the Cu/NBC showed better activity. The higher activity of these extracts and fractions might be associated with the number of bioactive metabolites and their synergetic activities.

Figure 7: Activity of the copper oxide nanoparticles and Cu/NBC extracts against E.coli and E.coli respectively.

4. CONCLUSION

In conclusion, Cu-modified NBC from spent coffee grounds was prepared by pyrolysis and subsequent acid digestion. The acid digestion method is simple and nanobiochar of size down to nanoscale. The resulting Cu-modified NBC was used as an effective adsorbent for phosphate removal and subsequent utility as an antibacterial agent. Batch mode adsorption studies showed phosphate adsorption on Cu/NBC followed pseudo-second-order kinetic and Freundlich isotherm models. The adsorption capacity was calculated to be 50.2 mg/g at 35 mg of Cu/NBC in 85 min at pH 3. Compared with other Cu-based biochar, the prepared Cu/NBC offered higher adsorption capacity. This is due to the increased effective surface area of the nanobiochar than its microsized counterparts. Cu/NBC showed better activity in the majority of test bacteria. The increased activity of this nanoparticle could be attributed to the presence of more bioactive metabolites and their synergistic effects.

5. CONFLICTS OF INTEREST

The authors declare that they have no conflicts of interest.

6. ACKNOWLEDGMENTS

The authors would like to thank the Mizan-Tepi University, Ethiopia for their support.

7. REFERENCES

1. Sisay GB, Atisme TB, Workie YA, Negie ZW, Mekonnen ML. Mg/Zr modified nanobiochar from spent coffee grounds for phosphate recovery and its application as a phosphorous release fertilizer. Environmental Nanotechnology, Monitoring & Management. 2023 May 1;19:100766. Available from: <URL>

2. Jiang D, Chu B, Amano Y, Machida M. Removal and recovery of phosphate from water by Mg-laden biochar: Batch and column studies. Colloids and Surfaces A: Physicochemical and Engineering Aspects. 2018 Dec 5;558:429-37. Available from: <URL>

3. Nobaharan K, Bagheri Novair S, Asgari Lajayer B, van Hullebusch ED. Phosphorus removal from wastewater: The potential use of biochar and the key controlling factors. Water. 2021 Feb 17;13(4):517. Available from: <URL>

4. Seo YI, Hong KH, Kim SH, Chang D, Lee KH, Do Kim Y. Phosphorus removal from wastewater by ionic exchange using a surface-modified Al alloy filter. Journal of Industrial and Engineering Chemistry. 2013 May 25;19(3):744-7. Available from: <URL>

5. Mbamba CK, Lindblom E, Flores-Alsina X, Tait S, Anderson S, Saagi R, Batstone DJ, Gernaey KV, Jeppsson U. Plant-wide model-based analysis of iron dosage strategies for chemical phosphorus removal in wastewater treatment systems. Water research. 2019 May 15;155:12-25. Available from: <URL>

6. Liu X, Shen F, Qi X. Adsorption recovery of phosphate from aqueous solution by CaO-biochar composites prepared from eggshell and rice straw. Science of the total environment. 2019 May 20;666:694-702. Available from: <URL>

7. Gusain R, Gupta K, Joshi P, Khatri OP. Adsorptive removal and photocatalytic degradation of organic pollutants using metal oxides and their composites: A comprehensive review. Advances in colloid and interface science. 2019 Oct 1;272:102009. Available from: <URL>

8. Huang W, Zhu Y, Tang J, Yu X, Wang X, Li D, Zhang Y. Lanthanum-doped ordered mesoporous hollow silica spheres as novel adsorbents for efficient phosphate removal. Journal of Materials Chemistry A. 2014;2(23):8839-48. Available from: <URL>

9. De Gisi S, Lofrano G, Grassi M, Notarnicola M. Characteristics and adsorption capacities of low-cost sorbents for wastewater treatment: A review. Sustainable Materials and Technologies. 2016 Sep 1;9:10-40. Available from: <URL>

10. Zhu D, Chen Y, Yang H, Wang S, Wang X, Zhang S, Chen H. Synthesis and characterization of magnesium oxide nanoparticle-containing biochar composites for efficient phosphorus removal from aqueous solution. Chemosphere. 2020 May 1;247:125847. Available from: <URL>

11. Kizito S, Wu S, Kirui WK, Lei M, Lu Q, Bah H, Dong R. Evaluation of slow pyrolyzed wood and rice husks

biochar for adsorption of ammonium nitrogen from piggery manure anaerobic digestate slurry. Science of the Total Environment. 2015 Feb 1;505:102-12. Available from: <URL>

12. Tavakoli S, Kharaziha M, Ahmadi S. Green synthesis and morphology dependent antibacterial activity of copper oxide nanoparticles. Journal of Nanostructures. 2019 Jan 1;9(1):163-71. Available from: <URL>

13. Kassaw S, Tamir A, Yimam BB. Phytochemical Investigation and Determination of Antibacterial Activities of the Fruit and Leaf Crude Extract of Ficus palmata. Sch Int J Chem Mater Sci. 2022;5(4):61-6. Available from: <URL>

14. Sisay GB, Mekonnen ML. Mg modified nanobiochar from spent coffee grounds: Evaluation of the phosphate removal efficiency and its application as a phosphorous release fertilizer. Chemistry Select. 2023; 8(47):e202302288. Available from: <URL>

15. Wang J, Guo X. Adsorption isotherm models: Classification, physical meaning, application and solving method. Chemosphere. 2020 Nov 1;258:127279. Available from: <URL>

16. Bekele T, Yimam BB. Phytochemical Screening and Antimicrobial Activity of Stem Bark Extracts of Schinus molle linens. Sch Int J Chem Mater Sci. 2023;6(5):108-14. Available from: <URL>

17. Melkamu WW, Feleke EG. Green Synthesis of Copper Oxide Nanoparticles Using Leaf Extract of Justicia Schimperiana and their Antibacterial Activity. Research Square. 2022. Available from: <URL>

18. Legesse BA, Tamir A, Bezabeh B. Phytochemical screening and antibacterial activity of leaf extracts of Dovyalis abyssinica. J Emerg Technol Innov Res. 2019;6(6):453-65.

19. Yin Q, Ren H, Wang R, Zhao Z. Evaluation of nitrate and phosphate adsorption on Al-modified biochar: influence of Al content. Science of the Total Environment. 2018 Aug 1;631:895-903. Available from: <URL>

20. Deng W, Zhang D, Zheng X, Ye X, Niu X, Lin Z, Fu M, Zhou S. Adsorption recovery of phosphate from waste streams by Ca/Mg-biochar synthesis from marble waste, calcium-rich sepiolite and bagasse. Journal of Cleaner Production. 2021 Mar 15;288:125638. Available from: <URL>

21. Shin H, Tiwari D, Kim, DJ. Phosphate adsorption/desorption kinetics and P bioavailability of Mg-biochar from ground coffee waste, Journal of Water Process Engineering. 2020;37: 101484. Available from: <URL>

22. Kim TH, Lundehøj L, Nielsen UG. An investigation of the phosphate removal mechanism by MgFe layered double hydroxides. Applied Clay Science. 2020;189:105521. Available from: <URL>

23. Humayro A, Harada H, Naito KJJOAC. Environment, adsorption of phosphate and nitrate using modified spent coffee ground and ıts application as an alternative nutrient source for plant growth. Journal of Agricultural Chemistry and Environment. 2020;10(1):80-90. Available from: <URL>